Wireless powered D2D communications underlying cellular networks: design and performance of the extended coverage

Hoang-Sy Nguyen, Thanh-Sang Nguyen & Miroslav Voznak

Published online: 04 May 2018.

Submit your article to this journal ↗

Article views: 676

View related articles ↗

View Crossmark data ↗

Taylor & Francis
Taylor & Francis Group

REGULAR PAPER

Wireless powered D2D communications underlying cellular networks: design and performance of the extended coverage

Hoang-Sy Nguyen [a], Thanh-Sang Nguyen[b,c] and Miroslav Voznak[b]

[a]Wireless Communications Research Group, Faculty of Electrical and Electronics Engineering, Ton Duc Thang University, Ho Chi Minh City, Vietnam; [b]Faculty of Electrical Engineering and Computer Science, Technical University of Ostrava, Ostrava-Poruba, Czech Republic; [c]Binh Duong University, Thu Dau Mot City, Binh Duong Province, Vietnam

ABSTRACT

Because of the short battery life of user equipments (UEs), and the requirements for better quality of service have been more demanding, energy efficiency (EE) has emerged to be important in device-to-device (D2D) communications. In this paper, we consider a scenario, in which D2D UEs in a half-duplex decode-and-forward cognitive D2D communication underlying a traditional cellular network harvest energy and communicate with each other by using the spectrum allocated by the base station (BS). In order to develop a practical design, we achieve the optimal time switching (TS) ratio for energy harvesting. Besides that, we derive closed-form expressions for outage probability, sum-bit error rate, average EE and instantaneous rate by considering the scenario when installing the BS near UEs or far from the UEs. Two communication types are enabled by TS-based protocol. Our numerical and simulation results prove that the data rate of the D2D communication can be significantly enhanced.

1. Introduction

In recent years, energy harvesting (EH), which is regarded as a promising technology in wireless communications, helps overcome the limitations of short network lifetime. In order to power wireless equipments, energy from both synthesized resources (i.e. microwave power transfer) and natural resources (i.e. wave, solar, wind, etc.) can be collected to transform into electricity [1–7]. In particular, the authors in [8] proposed two relaying protocols so-called time switching-based relaying (TSR) protocol and power splitting-based relaying (PSR) protocol to enable EH and information processing at the relay node. Following the work in [8], these authors continued evaluating the throughput performance and ergodic capacity of a decode-and-forward (DF) relaying network for both TSR and PSR protocols in [9]. In [10], the performance of two and three time slot transmission schemes in amplify-and-forward (AF) two-way relaying networks was investigated, where the authors proposed two new protocols: so-called power time splitting-based two-slot and power time splitting-based three-slot . Meanwhile, the authors in [10] continued their study on the throughput performance for two, three and four time slot transmission schemes for AF two-way relaying networks [11]. Regarding bit error rate (BER) performance, the sum BER performance of (AF) EH two-way relaying networks was evaluated deploying TSR protocol [12] while the work in [13] derived an exact

closed-form expression for average BER of a selection combining scheme for a cooperative system using an AF relay with simultaneous wireless information and power transfer.

There have been a number of works on cognitive radio networks (CRNs), where EH was mentioned in [14–17]. In [14], the resource-allocation problem for EH based on orthogonal frequency-division multiple access cooperative overlay CRNs was mentioned, where there was the involvement of multiple primary users (PUs) and secondary users (SUs), where they cooperate with each other with respect to information transmission and EH. In terms of small-cell CRNs, resource-allocation schemes for a CRN were investigated, where in different small cell PU networks, SUs establish communication with each other [15]. Furthermore, the authors in [16] focus on the power control and sensing time optimization problem in a small cell CRN, while a distributed sleep-mode strategy for cognitive small cell access points was addressed, and the trade-off between traffic offloading from the macro cell and the energy consumption of the small cells were also taken into consideration in [17].

Because of the demand of higher transmission rate and better spectral efficiency (SE), it contributes to the establishment of long-term evolution standards [18] and third generation partnership project [19]. In order to meet the requirements of the future communication, there is an increase in novel technologies, and among

---

CONTACT Hoang-Sy Nguyen nguyenhoangsy@tdt.edu.vn

them, device-to-device (D2D) communication has emerged as a promising technology. In [20], security aspect regarding D2D communication in EH large-scale CRNs was addressed, where expressions for the secrecy outage probability and the secrecy throughput were obtained to evaluate the secrecy performance, while the cognitive D2D transmitters harvest energy from ambient interference and use one of the channels allocated to cellular users (CUs) (in uplink or down-link) [21]. There have been several investigations on D2D communication underlying cellular networks. Particularly, the work in [22] focused on the optimization of the sum-rate of the D2D links without degrading the quality-of-service (QoS) requirement ofCUs. In [23], the closed-form expressions for average energy efficiency (EE) and SE of multi-hop D2D communications were provided.

Nevertheless, fixed relay location was solely discussed previous works, and spatial distribution at the relay user equipment (RUE), which impairs the outage performance and throughput of D2D communication, was neglected. Motivated from these limitations, we are going to study the D2D communication underlying a cellular network in case the location of base station (BS) is not fixed, and it is placed near UEs or far from UEs, so we can evaluate the system performance comprehensively.

The main contributions of this paper are summarized as follows:

- We consider a relay-assisted D2D communication underlying a cellular network, in which all nodes are restricted by the energy harvested from BS in the near distance and the peak interference power caused by CUs.
- The analytical closed-form expressions for outage probability and instantaneous rate are derived. We also achieve the optimal time switching (TS) ratio for EH. Besides that, the simulation results provide a comparison between the distance between BS and D2D user equipments. As a result, the closer the distance between BS and DUEs is, the better outage performance is improved compared to the direct D2D communication without spectrum sharing.
- EE in the considered system is evaluated, we can show the average for the energy efficient D2D communication based on different impacts of power circuits and transmission power, etc. In addition, the expression for the BER is also obtained.

We organize the paper as follows. We model the system and formulate the cooperation problem in Section 2. In Section 3, we derive the optimal TS for EH for the considered system and closed-form expressions for outage probability, the BER and the average

EE for the relay-assisted D2D communication are also provided. Simulation results and analysis are provided in Section 5. Section 6 draws a conclusion for the paper.

Notation

γ denotes signal-to-interference ratio (SIR) of specific links. $f_Z(.)$ and $F_Z(.)$ represent the probability distribution function (PDF) and the cumulative distribution function of random variables (RVs), Z, respectively. $Pr(.)$ is the outage probability function. $\mathbb{E}\{.\}$ denotes the expectation operation. $K_1(.)$ stands for the first-order modified Bessel function. $W(x)$ is the Lambert function. $W_{u,v}(x)$ is the Whitaker function. $Ei[.]$ is the exponential integral function.

2. System model

As depicted in Figure 1, we consider two communication types. In particular, a cellular network comprises a cellular equipment (CE) and a BS while a half-duplex (HD) relay-assisted cognitive D2D communication using DF consists of two D2D user equipments (i.e. DUE1 and DUE2) and a RUE, in which RUE is not only considered as a transmitter but it also assists the communication between the two DUE nodes due to the far distance between them. It is worth noting that the D2D communication is considered as an underlay to the cellular communication, where cellular spectrum resources are allocated by BS to the entire system thanks to the strength of BS. In conventional cellular networks, since BS transmits the intended signal to CE in the first coverage area, user equipments in the D2D communication suffer from interference stemming from the co-channel interference caused by the communication between BS and CE. Likewise, when RUE receives signals transmitted from DUE1, CE is affected by interference caused by the communication between the two D2D nodes.
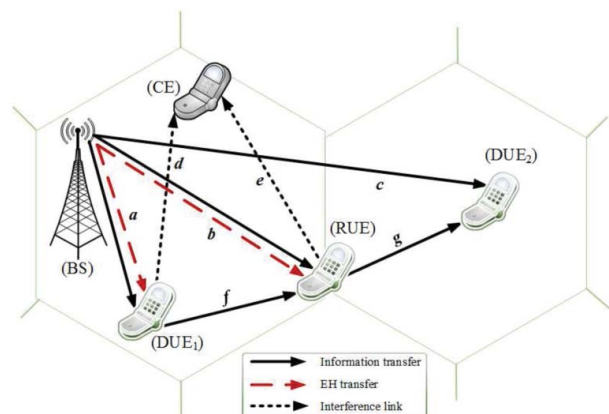

Figure 1. System model of energy harvesting-based cognitive D2D communications.
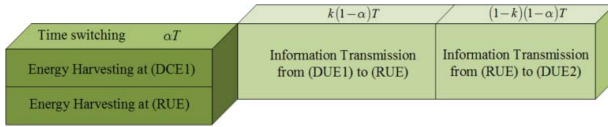
Figure 2. Time switching-based (TS) protocol for energy harvesting.

Meanwhile, the neighbouring cell only consists of DUE2, where DUE2 is placed further compared to DUE1, so RUE located between the two cells effectively assists the D2D links. In principle, the D2D links are considered to be reciprocal and stable, and they process in two equal consecutive time slots. It can be noted that all nodes are equipped with a single antenna, and the impact of noise is ignored.

In this paper, we deploy TS-based protocol to operate wireless power transfer at DUE1 and RUE. The harvested power controls the energy used by DUE1 and RUE over the transmission period denoted by E_S and E_R, respectively. As shown in Figure 2, DUE1 and RUE harvest energy for a period of αT, where T denotes the time block, and $0 < \alpha < 1$ is the TS fraction. After the amount of energy harvested at DUE1 and RUE is enough, DUE1 starts transmitting signals to RUE for a duration of $k(1 - \alpha)T$, then RUE forwards the transmitted signal to DUE2 for a duration of $(1 - k)(1 - \alpha)T$, where $k \in (0, 1)$ and assuming that $k = 1/2$. Additionally, the key of achieving better throughput is to find optimal α, so we consider that the impact of optimal α helps improve the throughput of D2D communications.

We denote r_a, r_b and r_c as the distances from BS to DUE1, RUE and DUE2, respectively while r_d and r_e are distances from CE to DUE1 and RUE, respectively. Regarding the D2D links, r_f and r_g are denoted as distances of DUE1-RUE link and RUE-DUE2 links, respectively.

Regarding the impact of the cellular communication, the wireless channels, a, b and c represent the channel gain coefficients of the control channels from BS to DUE1, RUE and DUE2, respectively while those from CE to DUE1 and RUE are denoted by d and e, respectively. Meanwhile, f and g denote as the channel gain coefficients from DUE1 to RUE and from RUE to DUE2, respectively. We assume flat-fading channels with path-loss and Rayleigh fading, and the channel coefficients remain for each signal frame but vary independently among various frames.

Without loss of generality, for each channel gain element, l_{ij} denotes as $i \rightarrow j$ link. Therefore, we derive the expression as follows [23]:

$$|l_{ij}|^2 = \frac{|l_0|^2}{PL_0 r_{ij}^m},\qquad(1)$$

where r_{ij} is the distance of $i \rightarrow j$ link, m is the path-loss exponent while PL_0 stands for the path-loss constant. The complex Gaussian RV is denoted as $|l_0|^2$ to model fading phenomena with mean, Ω_l for the l_{ij} link. Accordingly, the channel gains $|a_0|^2$, $|b_0|^2$, $|c_0|^2$, $|d_0|^2$, $|e_0|^2$, $|f_0|^2$ and $|g_0|^2$ follow an exponential distribution with parameters Ω_a, Ω_b, Ω_c, Ω_d, Ω_e, Ω_f and Ω_g, respectively.

The energy harvested at DUE1 and RUE considering TS protocol [9] can be expressed as

$$E_S = \left(\eta P_B \frac{|a_0|^2}{PL_a}\right) \times \alpha T,\qquad(2a)$$

and

$$E_R = \left(\eta P_B \frac{|b_0|^2}{PL_b}\right) \times \alpha T,\qquad(2b)$$

where $0 < \eta < 1$ is the energy conversion efficiency, and P_B is the transmit power of BS. The path-loss constant for BS-DUE1 link and BS-RUE link is denoted by $PL_a = PL_0 r_a^m$ and $PL_b = PL_0 r_b^m$, respectively.

In this proposed model, the transmit power from the D2D network can cause interference at the receiver of the cellular network, so a power constraint on the D2D network is imposed, in which its interference power cannot be higher than the peak interference power, P_D. To ensure the quality of D2D links, the transmit power at DUE1 and RUE must satisfy a constraint which is expressed as

$$P_S = \min\left(\frac{2E_S}{(1 - \alpha)T}, \frac{PL_d}{|d_0|^2}P_D\right),\qquad(3a)$$

and

$$P_R = \min\left(\frac{2E_R}{(1 - \alpha)T}, \frac{PL_e}{|e_0|^2}P_D\right),\qquad(3b)$$

where $PL_d = PL_0 r_d^m$ and $PL_e = PL_0 r_e^m$ are the path-loss constants for DUE1-CE link and RUE-CE link, respectively.

Following that, the signal-to-SIR at RUE and DUE2 is considered as independent RVs denoted by γ_R and γ_D for each node. Therefore, they can be expressed as

$$\gamma_R = \min\left(\delta\frac{|a_0|^2}{PL_a}P_B, \frac{PL_d}{|d_0|^2}P_D\right) \times \frac{PL_b|f_0|^2}{PL_f|b_0|^2 P_B},\qquad(4a)$$

and

$$\gamma_D = \min\left(\frac{|b_0|^2}{PL_b}\delta P_B, \frac{PL_e}{|e_0|^2}P_D\right) \times \frac{PL_c|g_0|^2}{PL_g|c_0|^2 P_B},\qquad(4b)$$

where $\delta = \frac{2\eta\alpha}{(1-\alpha)}$. $PL_c = PL_0 r_c^m$, $PL_f = PL_0 r_f^m$ and $PL_g = PL_0 r_g^m$ are the path-loss constants for BS-DUE2, DUE1-RUE and RUE-DUE2 links, respectively.

3. Energy harvesting protocol and performance analysis

In this part, we try to achieve the optimal TS ratio for BS-DUE1 link and expressions for outage probability. It is worth noting that the relay-assisted D2D communication is evaluated to derive the instantaneous SIR at RUE. Let us first present the optimal TS for instantaneous capacities at RUE.

3.1. Optimal time switching for instantaneous capacities at RUE

In this section, we consider the instantaneous capacities at RUE and evaluate the optimal TS, α. Thanks to the finding of optimal α which leads to the optimal transmit power at DUE1, throughput can be significantly enhanced.

From (4a), the SIR at RUE can be rewritten as

$$\gamma_{R_1} = \frac{\alpha}{(1-\alpha)} 2\eta \frac{|a_0|^2}{PL_a} \frac{|f_0|^2}{PL_f} \frac{PL_b}{|b_0|^2}, \quad (5a)$$

or

$$\gamma_{R_2} = \frac{P_D}{P_B} \frac{|f_0|^2}{PL_f} \frac{PL_b}{|b_0|^2} \frac{PL_d}{|d_0|^2}. \quad (5b)$$

Therefore, the instantaneous capacities at RUE can be computed by

$$\begin{aligned} R_{\text{RUE}}(\alpha) &= \frac{(1-\alpha)}{2} \log_2(1+\gamma_R) \\ &= \frac{(1-\alpha)}{2} \log_2\left(1 + \min(\gamma_{R_1}, \gamma_{R_2})\right) \end{aligned} \quad (6)$$

The following optimization needs to be solved before the optimal α can be achieved as follows: $\alpha^* \underset{0<\alpha<1}{=} \text{argmax}_\alpha R_{RUE}(\alpha)$.

Proposition 3.1: *The value of α can be expressed as*

$$\alpha^* = \begin{cases} \dfrac{\mu_2 - 1}{\mu_1 + \mu_2 - 1}, & \text{if} \quad \mu_2 < \mu_1 + 1 \\ \dfrac{1}{1 + \mu_3}, & \text{otherwise} \end{cases}, \quad (7)$$

where $\mu_1 = 2\eta \frac{|a_0|^2}{PL_a} \frac{|f_0|^2}{PL_f} \frac{PL_b}{|b_0|^2}$, $\mu_2 = e^{W\left(\frac{\mu_1-1}{e}\right)+1}$, and $\mu_3 = \frac{P_D PL_a PL_d}{2\eta P_B |a_0|^2 |d_0|^2}$.

Proof: It is noted that we have some definitions as follows: $\mu_1 = 2\eta \frac{|a_0|^2}{PL_a} \frac{|f_0|^2}{PL_f} \frac{PL_b}{|b_0|^2}$, $\mu_2 = \frac{P_D}{P_B} \frac{|f_0|^2}{PL_f} \frac{PL_b}{|b_0|^2} \frac{PL_d}{|d_0|^2}$, and $\psi^2 =$

$\mu_1 \mu_2$, respectively. Therefore, it is better to take two separate regions into consideration. Let us start with region 1, $0 < \alpha < \frac{1}{1+\psi}$. In case of region 1, we derive the instantaneous throughput as

$$R_{\text{RUE}} = \frac{(1-\alpha)}{2} \log_2\left(1 + \frac{\alpha}{1-\alpha}\mu_1\right). \quad (8)$$

We first let $\frac{dR_{\text{RUE}}(\alpha)}{d\alpha} = 0$ and take the first derivative of $R_{\text{RUE}}(\alpha)$ with respect to α. Thus, we have

$$\mu_1 + \frac{\alpha}{1-\alpha}\mu_1 = \left(1 + \frac{\alpha}{1-\alpha}\mu_1\right)\ln\left(1 + \frac{\alpha}{1-\alpha}\mu_1\right). \quad (9)$$

To this point, after some algebraic manipulations, we set $z = 1 + \frac{\alpha}{1-\alpha}\mu_1$. Therefore, we have

$$\alpha^* = \frac{z-1}{\mu_1 + z - 1}. \quad (10)$$

Thanks to the standard definition of Lambert function, W based on (9), we have

$$\ln\left(\frac{z}{e}\right) = W\left(\frac{\mu_1 - 1}{e}\right). \quad (11)$$

Then, let us define

$$z = e^{W\left(\frac{\mu_1-1}{e}\right)+1}. \quad (12)$$

Substituting (12) into (10), the result of α in the first region can be given by

$$\alpha^* = \frac{e^{W\left(\frac{\mu_1-1}{e}\right)+1} - 1}{\mu_1 + e^{W\left(\frac{\mu_1-1}{e}\right)+1} - 1}. \quad (13)$$

In terms of the second region, $\frac{1}{1+\psi} < \alpha < 1$. We take the first derivative, $R_{\text{RUE}}(\alpha)$ with respect to α which is a decreasing function with respect to α set below zero. Hence, we derive α as

$$\alpha^* = \frac{1}{1 + \frac{P_D PL_a PL_d}{2\eta P_B |a_0|^2 |d_0|^2}}. \quad (14)$$

To this end, the optimal α can be achieved in (13) or (14). This ends the proof for Proposition 3.1. □

Remark 3.1: It is worth noting that the evaluation of TS coefficient can be done with the constraint of α between 0 and 1 which indicates the best instantaneous capacities at RUE. Before achieving the best QoS (i.e. throughput), the RUE's pre-set power can be selected properly. Due to the RUE's dependence on α, the transmitted signal from RUE in each block is changeable, which relies on the quality of both D2D and cellular channels.

3.2. Outage probability

The outage probability in the relay-assisted D2D communication is represented by P_{out}, in which P_{out} is considered as the probability that the random values of SIR for each time slot (i.e. DUE1-RUE, RUE-DUE2) are set under a threshold value, γ_0. Consequently, the calculation of outage probability can be defined as

$$P_{\text{out}} = 1 - \Pr\{\gamma_R \geq \gamma_0, \gamma_D \geq \gamma_0\} \\ = 1 - \Pr\{\gamma_R \geq \gamma_0\} \times \Pr\{\gamma_D \geq \gamma_0\}. \tag{15}$$

We are going to derive the analytical closed-form expression for P_{out} in the following proposition.

Proposition 3.2: *The outage probability at DUE2 for DF transmission mode can be written as*

$$P_{\text{out}} = 1 - \Phi_1 \times (\Phi_2 + \Phi_3), \tag{16}$$

where

$$\Phi_1 = e^{\frac{1}{2}\psi_1} W_{-1,\frac{1}{2}}(\psi_1),$$

$$\Phi_2 = e^{\frac{1}{2}\psi_2} W_{-1,\frac{1}{2}}(\psi_2) - e^{\frac{1}{2}\psi_2} W_{-1,\frac{1}{2}}(\psi_2)\sqrt{\psi_3}K_1\left(\sqrt{\psi_3}\right),$$

$$\Phi_3 = \psi_3\psi_4 e^{\psi_4} E_1(\psi_4)K_1(\psi_3),$$

$$\psi_1 = \frac{PL_a PL_f \Omega_b \gamma_0}{PL_b \Omega_a \Omega_f \delta}, \ \psi_2 = \frac{PL_b PL_g \Omega_c \gamma_0}{PL_c \Omega_b \Omega_g \delta},$$

$$\psi_3 = 2\sqrt{\frac{PL_b PL_e P_D}{\Omega_e \Omega_b \delta P_B}}, \ and \ \psi_4 = \frac{PL_c PL_e \Omega_g P_D}{PL_g \Omega_c \Omega_e P_B \gamma_0}.$$

Proof: Let us first compute the probability related to SIR at RUE when conditioning $\Phi_1 = \Pr\{\gamma_R \geq \gamma_0\}$ on b_0 as $\Phi_1 = \Pr\left\{|f_0|^2 \geq \frac{PL_f PL_a |b_0|^2 \gamma_0}{PL_b |a_0|^2 \delta}\right\}$.

Hence, the cumulative distribution function (CDF) of γ_R can be given by

$$\Phi_1 | |b_0|^2 = \frac{1}{\Omega_a}\int_{x=0}^{\infty} e^{-\frac{1}{x}\left(\frac{PL_a PL_f |b_0|^2 \gamma_0}{PL_b \Omega_f \delta}\right) - \frac{x}{\Omega_a}} dx \\ = 2\sqrt{\frac{PL_a PL_f |b_0|^2 \gamma_0}{PL_b \Omega_a \Omega_f \delta}}K_1\left(2\sqrt{\frac{PL_a PL_f |b_0|^2 \gamma_0}{PL_b \Omega_a \Omega_f \delta}}\right). \tag{17}$$

Consequently, the result over the distribution of b_0 is achieved as follows:

$$\Phi_1 = \frac{1}{\Omega_b}\int_{y=0}^{\infty} 2e^{-\frac{y}{\Omega_b}}\sqrt{\frac{PL_a PL_f \gamma_0}{PL_b \Omega_a \Omega_f \delta}}yK_1\left(2\sqrt{\frac{PL_a PL_f \gamma_0}{PL_b \Omega_a \Omega_f \delta}}y\right)dy \\ = e^{\frac{1}{2}\left(\frac{PL_a PL_f \Omega_b \gamma_0}{PL_b \Omega_a \Omega_f \delta}\right)} W_{-1,\frac{1}{2}}\left(\frac{PL_a PL_f \Omega_b \gamma_0}{PL_b \Omega_a \Omega_f \delta}\right), \tag{18}$$

thanks to the use of formula (3.324.1) and (6.643.3) in [24].

The probability term for SIR at DUE2 can be obtained in the same situation as

$$\Pr\{\gamma_D \geq \gamma_0\} \\ = \Pr\left\{\min\left(\frac{|b_0|^2}{PL_b}\delta P_B, \frac{PL_e}{|e_0|^2}P_D\right)\frac{PL_c|g_0|^2}{PL_g|c_0|^2 P_B} \geq \gamma_0\right\} \\ = \underbrace{\Pr\left\{|g_0|^2 \geq \frac{PL_b PL_g |c_0|^2 \gamma_0}{PL_c|b_0|^2\delta}, |e_0|^2 \leq \frac{PL_b PL_e P_D}{|b_0|^2\delta P_B}\right\}}_{\Phi_2} \\ + \underbrace{\Pr\left\{|g_0|^2 \geq \frac{PL_g|c_0|^2|e_0|^2 P_B\gamma_0}{PL_c PL_e P_D}, |e_0|^2 \geq \frac{PL_b PL_e P_D}{|b_0|^2\delta P_B}\right\}}_{\Phi_3}. \tag{19}$$

Then, the left joint probability in the above expression can be derived by the product of two independent probabilities as $\Phi_2 = \Pr\{|g_0|^2 \geq \frac{PL_b PL_g|c_0|^2\gamma_0}{PL_c|b_0|^2\delta}\} \times \Pr\{|e_0|^2 \leq \frac{PL_b PL_e P_D}{|b_0|^2\delta P_B}\}$.

Similarly, before the left term is expressed, $\Phi_{2,a}$ must be conditioned on c_0. Therefore, we have

$$\Phi_{2,a}||c_0|^2 = \frac{1}{\Omega_b}\int_{x=0}^{\infty} e^{-\frac{1}{x}\left(\frac{PL_b PL_g|c_0|^2\gamma_0}{PL_c \Omega_g \delta}\right) - \frac{x}{\Omega_b}} dx \\ = 2\sqrt{\frac{PL_b PL_g|c_0|^2\gamma_0}{PL_c \Omega_b \Omega_g \delta}}K_1\left(2\sqrt{\frac{PL_b PL_g|c_0|^2\gamma_0}{PL_c \Omega_b \Omega_g \delta}}\right). \tag{20}$$

Afterwards, we derive a new expression over the distribution of c_0 as

$$\Phi_{2,a} \\ = \frac{1}{\Omega_c}\int_{y=0}^{\infty} 2e^{-\frac{y}{\Omega_c}}\sqrt{\frac{PL_b PL_g \gamma_0}{PL_c \Omega_b \Omega_g \delta}}yK_1\left(2\sqrt{\frac{PL_b PL_g \gamma_0}{PL_c \Omega_b \Omega_g \delta}}y\right)dy \\ = e^{\frac{1}{2}\left(\frac{PL_b PL_g \Omega_c\gamma_0}{PL_c \Omega_b \Omega_g \delta}\right)} W_{-1,\frac{1}{2}}\left(\frac{PL_b PL_g \Omega_c\gamma_0}{PL_c \Omega_b \Omega_g \delta}\right). \tag{21}$$

Likewise, the right term, $\Phi_{2,b}$ is presented by

$$\Phi_{2,b} = 1 - \frac{1}{\Omega_b}\int_{x=0}^{\infty} e^{-\frac{1}{x}\left(\frac{PL_b PL_e P_D}{\Omega_e \delta P_B}\right) - \frac{x}{\Omega_b}} dx \\ = 1 - \sqrt{\frac{4PL_b PL_e P_D}{\Omega_b \Omega_e \delta P_B}}K_1\left(\sqrt{\frac{4PL_b PL_e P_D}{\Omega_b \Omega_e \delta P_B}}\right). \tag{22}$$

In the same manner, based on (19), the right joint probability in the above expression can be obtained by the product of two independent probabilities $\Phi_3 = \Pr\left\{|g_0|^2 \geq PL_g|c_0|^2\frac{|e_0|^2 P_B\gamma_0}{PL_c PL_e P_D}\right\} \times \Pr\left\{|e_0|^2 \geq \frac{PL_b PL_e P_D}{|b_0|^2\delta P_B}\right\}$.

Following that, the left term, $\Phi_{3,a}$ on e_0 can be computed as

$$
\Phi_{3,a}||e_0|^2 = \frac{1}{\Omega_c} \int_{x=0}^{\infty} e^{-x\left(\frac{PL_g|e_0|^2 P_B\gamma_0}{PL_c PL_e \Omega_g P_D} + \frac{1}{\Omega_c}\right)} dx
$$
$$
= \frac{PL_c PL_e \Omega_g P_D}{PL_g \Omega_c P_B \gamma_0} \left(\frac{1}{\frac{PL_c PL_e \Omega_g P_D}{PL_g \Omega_c P_B \gamma_0} + |e_0|^2} \right).
$$
(23)

The average value of $\Phi_{3,\,a}$ over the PDF e_0 can be calculated as

$$
\Phi_{3,a} = \frac{\phi}{\Omega_e} \int_{y=0}^{\infty} \left(\frac{1}{\phi+y}\right) e^{-\frac{y}{\Omega_e}} dy
$$
$$
= -\frac{\phi}{\Omega_e} e^{\frac{\phi}{\Omega_e}} Ei\left(-\frac{\phi}{\Omega_e}\right),
$$
(24)

where $\phi = \frac{PL_c PL_e \Omega_g P_D}{PL_g \Omega_c P_B \gamma_0}$ and we apply ([24],3.352.4).
The probability, $\Phi_{3,\,b}$ of the right term can be given based on (22):

$$
\Phi_{3,b} = \Pr\left\{ |e_0|^2 \geq \frac{PL_b PL_e P_D}{|b_0|^2 \delta P_B} \right\} = 1 - \Phi_{2,b}
$$
$$
= 2\sqrt{\frac{PL_b PL_e P_D}{\Omega_b \Omega_e \delta P_B}} K_1\left(2\sqrt{\frac{PL_b PL_e P_D}{\Omega_b \Omega_e \delta P_B}}\right) \qquad . \quad (25)
$$

Eventually, we can prove the Proposition 3.1 by using (18), (21), (22), (24) and (25). □

3.3. Performance analysis

To analyse the system performance, clarifying the channel state information (CSI) in D2D networks is important. It is assumed that CSI is available at DUE2. In terms of the calculation of the instantaneous rate, it should be computed by the global instantaneous CSI. In principle, the instantaneous rate at RUE and DUE2 can be computed by

$$
R_i \underset{i\in(R,D)}{=} \frac{1}{2}\beta(1-\alpha)\log_2(1+\gamma_i),
$$
(26)

where β is denoted as the signal bandwidth, and SIR at RUE and DUE2 as γ_R, γ_D defined in (6) and (7), respectively.

The sum-BER, B_s is considered as the sum of the BER at RUE and DUE. Before we derive the expressions for sum-BER, the sum-symbol error rate must be taken into consideration first [25]. The expression for sum-BER can be given by

$$
B_s = \sum_{i\in\{R,D\}} \mathbb{E}\left[aQ\left(\sqrt{2b\gamma_i}\right)\right],
$$
(27)

where modulation-specific constants are denoted by a, b, and $Q(x) = \frac{1}{\sqrt{2\pi}} \int_x^{\infty} e^{-\frac{y^2}{2}} dy$ is the Gaussian function. It can be noted that these modulation formats involve BPSK ($a = 1$, $b = 1$), BFSK with orthogonal signalling ($a = 1$, $b = 0.5$) [26].

The expression of sum-BER in (31) can be given directly in terms of outage probability at RUE and DUE by applying integration by parts as

$$
B_s = \sum_{i\in\{R,D\}} \frac{a\sqrt{b}}{2\sqrt{\pi}} \int_{x=0}^{\infty} \frac{e^{-bx}}{\sqrt{x}} F_{\gamma_i}(x) dx,
$$
(28)

where based on Proposition 3.2, we redefine the instantaneous outage probability expression at RUE and DUE as $F_{\gamma_R}(x) = 1 - \Phi_1$, $F_{\gamma_D}(x) = 1 - (\Phi_2 + \Phi_3)$, respectively, with

$$
\Phi_1 = e^{\frac{1}{2}\psi_1} W_{-1,\frac{1}{2}}(\psi_1),
$$
$$
\Phi_2 = e^{\frac{1}{2}\psi_2} W_{-1,\frac{1}{2}}(\psi_2) - e^{\frac{1}{2}\psi_2} W_{-1,\frac{1}{2}}(\psi_2)\sqrt{\psi_3} K_1\left(\sqrt{\psi_3}\right),
$$
$$
\Phi_3 = \psi_3 \psi_4 e^{\psi_4} E_1(\psi_4) K_1(\psi_3),
$$
$$
\psi_1 = \frac{PL_a PL_f \Omega_b x}{PL_b \Omega_a \Omega_f \delta}, \ \psi_2 = \frac{PL_b PL_g \Omega_c x}{PL_c \Omega_b \Omega_g \delta},
$$
$$
\psi_3 = 2\sqrt{\frac{PL_b PL_e P_D}{\Omega_e \Omega_b \delta P_B}}, \text{ and } \psi_4 = \frac{PL_c PL_e \Omega_g P_D}{PL_g \Omega_c \Omega_e P_B x}.
$$

The sum-BER is given following the fading channels 2. Despite the difficulties in achieving closed-form expressions for the instantaneous sum-BER, its performance is going to be evaluated by using Monte Carlo simulations in the following section.

Furthermore, we use an EE metric to evaluate the performance of the system, such as the system throughput [22]. In this scenario, there are two aspects of energy consumption, including power transmission for reliable data transmission and the circuit energy consumption. The average EE denoted as n_{ee} can be calculated by

$$
n_{ee} = \frac{\sum_{i\in\{R,D\}} (1-\alpha)\mathbb{E}\left\{\log_2(1+\gamma_i)\right\}}{2P_{total}},
$$
(29)

where $P_{total} = P_S + P_R + 2P_C$, and P_C is constant which stands for the associated circuit energy consumption at all UEs.

4. Numerical results

In this section, we use the closed-form expression for the outage probability to evaluate the system performance. Furthermore, with the impact of EH period, α and the transmit power of BS, P_B, we can derive the best D2D communication performance in order to find the most acceptable distance between UEs and the BS. We assume that the network topology is designed at various locations denoted by two dimensions (x, y).
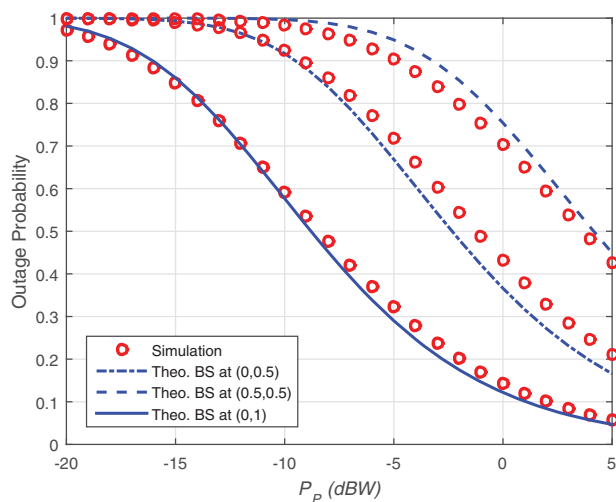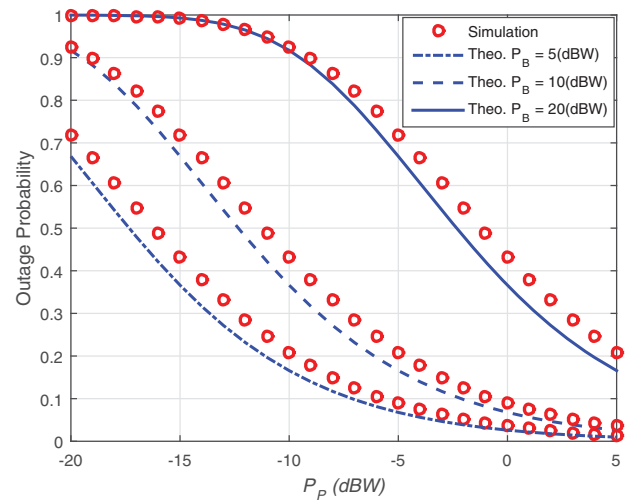
Table 1. Simulation parameters.

Parameters	Value
Channel bandwidth	$\beta = 10$ MHz
The circuit power	$P_C = 0$ dBW
The transmit power at BS,	$P_B = 20$ dBW
The SIR	$\gamma_0 = 0$ dBW
The energy efficiency	$\eta = 0.4$
The mean of all channel gain coefficients	$\Omega_a = \Omega_b = \Omega_c = \Omega_d = \Omega_e = \Omega_f = \Omega_g = \Omega = 5$
The BS is located at	$(0, 0.5)$
The CE is located at	$(1, 0.5)$
The DUE1, RUE and DUE2 are located at	$(0, 0)$, $(0.5, 0)$ and $(1, 0)$, respectively
The path loss for the D2D link, $i \rightarrow j$	$PL_0 = 148 + 40\log_{10}[r_{ij}(\text{km})]$dB

Note that the simulation results between the Monte Carlo simulation points marked as "⊙" are averaged over 10^5 channel realizations.

Main simulation parameters and their default values are listed in Table 1 for simplicity. Note that some parameters' values can be changed due to various conditions based on [19,23].

According to Figure 3, it illustrates the transmit power at BS, P_B versus the outage probability at DUE1, when $\gamma_0 = 0$ dB, the equivalent optimal α and the peak interference power, $P_D = 5$(dBW). We simulate the locations of three nodes as $(0, 0.5)$, $(0.5, 0.5)$ and $(1, 0)$ to define the distance between BS and the two considered communication types. As BS spends α to transmit energy, the location of BS is nearly between DUE1 and DUE2, at $(0.5, 0.5)$, the outage performance of this scenario outperforms that in case BS is close to DUE1. Additionally, if these nodes are moved further, the less energy will be allocated to them.

The outage probability versus the transmit power at BS is presented in Figure 4 in case BS is at $(0, 0.5)$ under the impact of different values of peak interference power, P_D. If P_D increases, the outage probability is lower. It is obvious that higher transmit power at BS and DUE1 is enabled by higher P_D, and hence this leads to lower outage probability. When P_B increases, the outage probability curves to the left. This situation can be explained as follows. First, as P_B increases,

Figure 4. Outage probability versus P_P with difference power constraints P_D.

DUE1 and RUE transmit with higher power to implement the interference from BS. Second, when P_D increases, the transmit power at DUE1 and RUE is restricted, by that way P_B can enable DUE1 and RUE to transmit at higher levels of power without crossing P_D.

Figure 5 considers outage probability versus the SIR threshold γ_0 and we use some parameters (i.e. $P_B = 20$ at $(0, 0.5)$, and $P_D = 5$ at $(0, 0.5)$) for two cases. In
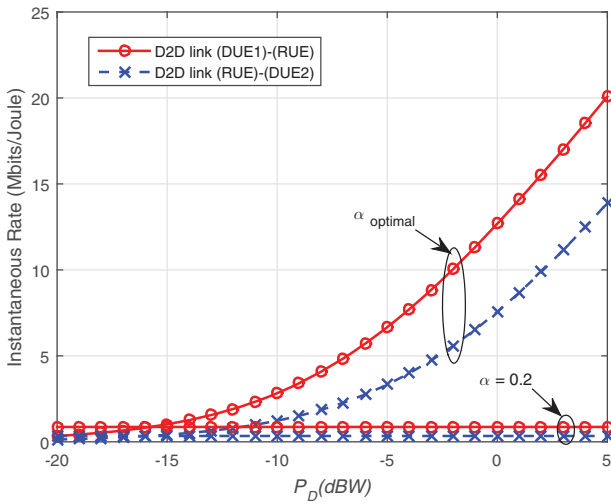

Figure 3. Outage probability versus P_P.
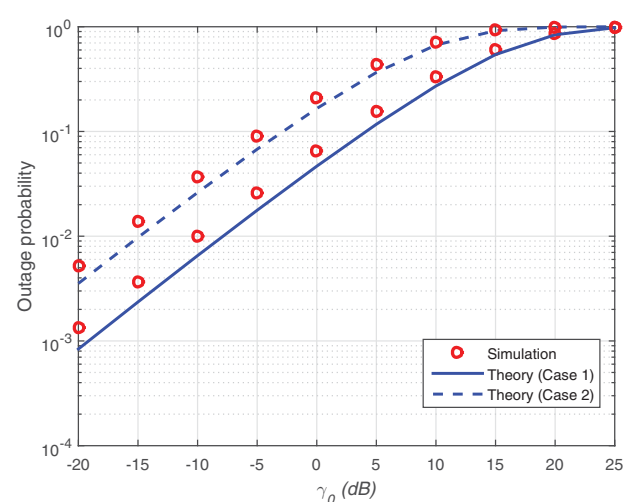
Figure 5. Outage probability versus γ_0 in two cases.

Figure 6. Instantaneous rate versus P_D (dBW) with α.

Figure 8. Sum-bit error rate versus P_D (dBW).

particular, Cases 1 and 2 are represented as $\Omega = 1$ and $\Omega = 5$, respectively. It is clear that when there is an increase in γ_0, the outage probability in the D2D communication falls. For each given value of γ_0, the channel gain coefficients decrease as the outage probability rises.

As illustrated in Figure 6, the instantaneous rate of each link in the D2D communication (i.e. DUE1-RUE, RUE-DUE2), as a function of P_D. It is clear that the optimal α along with P_D will rise, leading to the rise in the SIR. Consequently, the data rate is improved compared to that in case $\alpha = 0.2$. Note that the optimal α of the instantaneous rate of DUE1-RUE link is twice or half better than that of RUE-DUE2 link, because the transmit power at DUE1 can reach the optimal value.

Figure 7 presents the average EE with the parameters used above for the impact of three different values of energy conversion efficiency, (i.e. $\eta = 0.8$, $\eta = 0.4$, $\eta = 0.1$). In particular, the average EE rises along with P_D to the highest level before decreasing to
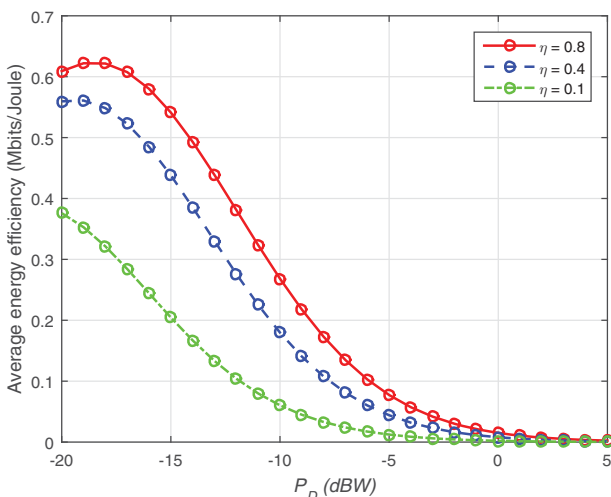
approximately 18(dB) as there is an increase in P_D. Furthermore, the energy scavenged is less sensitive to P_D than η. The average EE is linear with η, η has an impact on the transmitted signal in the D2D communication.

In Figure 8, the sum-BER is depicted as a function of P_D, where we set two different values of α (optimal α and $\alpha = 0.2$). It can be noted that the optimal value of α at DUE1 enjoys lower sum-BER compared to the system with fixed value, $\alpha = 0.2$, which also leads to the stable values of sum-BER over the given period while the figure for α decreases gradually.

5. Conclusion

In this paper, we considered a combination of a HD DF cognitive relay-assisted D2D communication underlying a traditional cellular network, in which D2D user equipments operate in HD transmission mode. We achieved the optimal TS for EH to guarantee the quality for the D2D links. Additionally, closed-form expressions for outage probability, average EE, sum-BER and instantaneous rate were provided. More importantly, with the help of EH, the data rate in the D2D communication can support the enhancement of the link robustness. We also provide numerical and simulation outcomes to prove our theoretical analysis and the impact of system settings on the performance were taken into consideration.

Figure 7. Average energy efficiency with P_D (dBW) versus different values of P_B and η.

Disclosure statement

No potential conflict of interest was reported by the author.

ORCID

Hoang-Sy Nguyen ⓘ http://orcid.org/0000-0002-1547-8416

References

[1] Liu J, Xiong K, Fan P, et al. RF energy harvesting wireless powered sensor networks for smart cities. IEEE Access. 2017;5:9348–9358.

[2] Do D-T, Nguyen H-S, Voznak M, et al. Wireless powered relaying networks under imperfect channel state information: system performance and optimal policy for instantaneous rate. Radioengineering. 2017;26 (3):869–877.

[3] Sakr AH, Hossain E,. Cognitive and energy harvesting-based D2D communication in cellular networks: stochastic geometry modeling and analysis. IEEE Trans Commun. 2015;63(5):1867–1880.

[4] Yao F, Wu H, Chen Y, et al. Cluster-based collaborative spectrum sensing for energy harvesting cognitive wireless communication network. IEEE Access. 2017;5:9266–9276.

[5] Tang L, Zhang X, Zhu P, et al. Wireless information and energy transfer in fading relay channels. IEEE J Sel Areas Commun. 2016;34(12):3632–3645.

[6] Joo C, Kang S,. Joint scheduling of data transmission and wireless power transfer in multi-channel device-to-device networks. J Commun Netw. 2017;19(2):180–188.

[7] Nguyen H-S, Do D-T, Nguyen T-S, et al. Exploiting hybrid time switching-based and power splitting-based relaying protocol in wireless powered communication networks with outdated channel state information. Automatika. 2017;58(1):111–118.

[8] Nasir AA, Zhou X, Durrani S, et al. Relaying protocols for wireless energy harvesting and information processing. IEEE Trans Wireless Commun. 2013;12 (7):3622–3636.

[9] Nasir AA, Zhou X, Durrani S, et al. Throughput and ergodic capacity of wireless energy harvesting based DF relaying network. In: IEEE, editor. Proceeding of the IEEE International Conference on Communications (ICC). Sydney, NSW, Australia; 2014. p. 4066–4071.

[10] Nguyen H-S, Do D, Voznak M. Two-way relaying networks in green communications for 5G: optimal throughput and trade-off between relay distance on power splitting-based and time switching-based relaying SWIPT. AEU – Int J Electron Commun. 2016;70 (12):1637–1644.

[11] Nguyen H-S, Do D-T, Bui A-H, et al. Self-powered wireless two-way relaying networks: model and throughput performance with three practical schemes. Wirel Pers Commun. 2017;97(1):613–631.

[12] Huang C, Sadeghi P, Nasir AA. BER performance analysis and optimization for energy harvesting two-way relay networks. In: IEEE, editor. Communications Theory Workshop; Melbourne, VIC, Australia; 2016. p. 20–22.

[13] Lou Y, Yu Q-Y, Cheng J, et al. Exact BER analysis of selection combining for differential SWIPT relaying systems. IEEE Signal Process Lett. 2017;24(8):1198–1202.

[14] Wang F, Zhang X. Resource allocation for multiuser cooperative overlay cognitive radio networks with RF energy harvesting capability. In: IEEE, editor. Proceeding of Global Communications Conference (GLOBECOM); Washington (DC); 2016. p. 1–6.

[15] Mallick S, Devarajan R, Loodaricheh RA, et al. Robust resource optimization for cooperative cognitive radio networks with imperfect CSI. IEEE Trans Wirel Commun. 2015;14(2):907–920.

[16] Zhang H, Nie Y, Cheng J, et al. Sensing time optimization and power control for energy efficient cognitive small cell with imperfect hybrid spectrum sensing. IEEE Trans Wirel Commun. 2017;16(2):730–743.

[17] Wildemeersch M, Quek TQS, Slump CH, et al. Cognitive small cell networks: energy efficiency and trade-offs. IEEE Trans Commun. 2013;61(9):4016–4029.

[18] Polak L, Kaller O, Klozar L, et al. Influence of the LTE system using cognitive radio technology on the DVB-T2 system using diversity technique. Automatika. 2016;57(2):496–505.

[19] TSG-RAN G. Further advancements for E-Utra physical layer aspects. 2010. (3GPP Technical Report, 3G TR 36.814 v9.0.0).

[20] Liu Y, Wang L, Zaidi SAR, et al. Secure D2D communication in large-scale cognitive cellular networks: a wireless power transfer model. IEEE Trans Commun. 2016;64(1):329–342.

[21] Sakr AH, Hossain E. Cognitive and energy harvesting-based D2D communication in cellular networks: stochastic geometry modeling and analysis. IEEE Trans Commun. 2015;63(5):1867–1880.

[22] Gupta S, Zhang R, Hanzo L. Energy harvesting aided device-to-device communication underlaying the cellular downlink. IEEE Access. 2016;5:7405–7413.

[23] Wei L, Hu RQ, Qian Y, et al. Energy efficiency and spectrum efficiency of multihop device-to-device communications underlaying cellular networks. IEEE Trans Veh Technol. 2016;65:367–380.

[24] Gradshteyn IS, Ryzhik IM. Table of integrals, series, and products. 4th ed. Academic Press, Inc.; 1980.

[25] Goldsmith AJ. Wireless communications. Cambridge (UK): Cambridge University Press; 2005.

[26] Simon MK, Alouini M-S. Digital communications over fading channels: a unified approach to performance analysis. 1st ed. New York (NY): Wiley; 2000.